

EFDA–JET–PR(12)16

HT. Kim, A.C.C. Sips
and JET EFDA contributors

Criterion for Plasma Burn-Through in Tokamaks

“This document is intended for publication in the open literature. It is made available on the understanding that it may not be further circulated and extracts or references may not be published prior to publication of the original when applicable, or without the consent of the Publications Officer, EFDA, Culham Science Centre, Abingdon, Oxon, OX14 3DB, UK.”

“Enquiries about Copyright and reproduction should be addressed to the Publications Officer, EFDA, Culham Science Centre, Abingdon, Oxon, OX14 3DB, UK.”

The contents of this preprint and all other JET EFDA Preprints and Conference Papers are available to view online free at www.iop.org/Jet. This site has full search facilities and e-mail alert options. The diagrams contained within the PDFs on this site are hyperlinked from the year 1996 onwards.

Criterion for Plasma Burn-Through in Tokamaks

HT. Kim¹, A.C.C. Sips²
and JET EFDA contributors*

JET-EFDA, Culham Science Centre, OX14 3DB, Abingdon, UK

¹*Department of Physics, Imperial College London, Prince Consort Road, London, SW7 2AZ, UK*
²*EURATOM-CCFE Fusion Association, Culham Science Centre, OX14 3DB, Abingdon, OXON, UK*

** See annex of F. Romanelli et al, "Overview of JET Results",
(23rd IAEA Fusion Energy Conference, Daejeon, Republic of Korea (2010)).*

Preprint of Paper to be submitted for publication in
Plasma Physics and Controlled Fusion

ABSTRACT.

Key aspects of physics for plasma burn-through in tokamaks are investigated with DYON code, modelling the plasma formation during the initiation phase of tokamak discharge. The simulation results are explained with the Radiation and Ionization Barrier (RIB) and the Critical Degree of Ionization $\gamma(t_{\text{RIB}})$, obtained by an analytical derivation. The required electric field for plasma burn-through, the burn-through criterion, is compared to the Townsend Avalanche Criterion, and the resultant operation space available for plasma formation in Joint European Torus (JET) is presented.

1. Introduction

Tokamak start-up consists of the plasma break-down phase, the plasma burn-through phase, and the ramp-up phase of plasma current I_p [1].

The Townsend avalanche theory[2][3] is generally used to calculate the required electric field for plasma break-down at a given prefill gas pressure and effective connection length as shown below,

$$E \geq \frac{1.25 \times 10^4 p}{\ln(510pL_f)}, \quad (1.1)$$

where L_f and p are the effective connection length along the magnetic field lines and the prefill gas pressure of the vacuum vessel, respectively. The required electric field for plasma break-down in International Thermonuclear Experimental Reactor (ITER) has also been calculated with the Townsend criterion in [1].

However, the Townsend avalanche theory is not sufficient to explain non-sustained break-down discharges where I_p does not increase as it specifies the condition for electron avalanche. In order for I_p to increase, sufficient ionization of prefill gas(deuterium), the plasma burn-through, is necessary. Otherwise, most heating power is lost through radiation and ionizations of the remaining neutrals, so that it prevents electron temperature from increasing in the I_p ramp-up phase[2].

The required loop voltage for plasma burn-through, the burn-through criterion, is generally higher than that for plasma break-down in present tokamaks[1]. Therefore, when designing a new device or determining the operation space, the burn-through criterion must be considered as well as the Townsend criterion. In 2009, more than 100 shots in Joint European Torus (JET) failed during the burn-through phase. These start-up failures can be prevented by understanding key physics aspects of the burn-through phase.

Furthermore, for ITER start-up, due to the engineering issues resulting from the use of superconducting central solenoid coils and a continuous vacuum vessel, the allowable toroidal electric field is limited up to $0.35[V/m]$ [4]. Tokamak start-up using a low electric field limits the operation space available of prefill gas pressure, magnetic error fields, and impurity content[5]. For reliable start-up using a low electric field, ECH-assisted start-up is planned in ITER[4]. The required ECH power can be estimated by understanding the burn-through conditions (or requirements).

Despite the increasing importance of the burn-through criterion, the theoretical investigation has not been published extensively since the complicated plasma surface interaction during the burn-through phase makes a theoretical approach difficult. For the sake of simplicity, uniform temperature and density (0D treatment) and pure deuterium plasma (no impurity) are assumed to investigate the criterion for plasma burn-through. Under the given assumptions, the key aspects of physics determining whether I_p increases are investigated using the DYON code[6] in section 2, and the Radiation and Ionization Barrier(RIB) and the critical degree of ionization $\gamma(t_{RIB})$, determining the criterion for plasma burn-through, are derived in section 3. In section 4, the effects of prefill gas pressure and impurities on plasma burn-through are investigated, and the criterion for plasma burn-through in JET, computed with the DYON code, are compared to the Townsend Avalanche Criterion. Section 5 provides conclusions.

2. Conditions for Plasma Current Ramp-up

The DYON code[6], a new plasma burn-through model, has been used for the numerical calculations presented in this article. The plasma parameters assumed in the simulation are given in Table 1. The initial degree of ionization is calculated to be 0.002 according to [6][7]. In order to simulate both successful I_p ramp-up and failure cases, two different prefill gas pressures are assumed, $5 \times 10^{-5}[Torr]$ (Success), and $7 \times 10^{-5}[Torr]$ (Failure) as shown in Figures 1, 2, and 4.

The plasma current I_p can be calculated with the circuit equation

$$I_p = \frac{1}{R_p}(V_l - L_p \frac{dI_p}{dt}) \quad (2.1)$$

where R_p , V_l , and L_p are the plasma resistance, the loop voltage, and the plasma inductance, respectively. In order for I_p to increase for a given V_l , which is approximately constant in the I_p ramp-up phase, R_p must be decreasing. According to Spitzer resistivity, R_p decreases with increasing electron temperature T_e [8], i.e. $R_p \propto T_e^{-\frac{3}{2}}$. Therefore,

$$\frac{dT_e}{dt} > 0 \quad (2.2)$$

is a necessary condition for I_p ramp-up.

Whether or not T_e increases is determined by the equation of electron energy balance,

$$P_e = \frac{3}{2} \frac{d(n_e e T_e)}{dt} = \frac{3}{2} e T_e \frac{dn_e}{dt} + \frac{3}{2} e n_e \frac{dT_e}{dt}, \quad (2.3)$$

where P_e is the net electron heating power, determined by the ohmic heating power P_{Oh} and the total electron power loss P_{Loss} , i.e. $P_e = P_{Oh} - P_{Loss}$. As separated into the two terms in Equation (2.3), the net electron heating power P_e is consumed by increasing n_e or T_e , i.e. $\frac{3}{2} e T_e \frac{dn_e}{dt}$ or $\frac{3}{2} e n_e \frac{dT_e}{dt}$.

Figure 1(a) describes the simulation result of the power consumption for successful I_p ramp-up(blue) and failed(red), and Figure 1(b) indicates the corresponding plasma

currents. As shown, P_e is positive for the successful case, and goes to zero in the failed case during the I_p ramp-up phase. Whereas the power consumed by the increasing n_e (chain lines) is dominant in the burn-through phase, it is small enough to be ignored in the I_p ramp-up phase as shown in Figure 1(a). Therefore, P_e in the I_p ramp-up phase can be approximated to be $P_e \approx \frac{3}{2}en_e \frac{dT_e}{dt}$. Accordingly, in order for T_e increases, P_e must be positive in the I_p ramp-up phase, i.e.

$$P_e > 0. \quad (2.4)$$

In this simulation, the deuterium recycling coefficient Y_D^D is assumed as 1. In the case that Y_D^D is higher than 1, the power consumed by the increasing n_e would be somewhat higher than 0. However, Equation (2.4) is still a necessary condition for the increase in T_e unless the power consumed by the increasing n_e exceeds P_e .

Figure 2 shows P_{Oh} and P_{Loss} in the cases of I_p ramp-up success (blue) and failure (red), respectively. In the successful case, P_{Oh} (blue solid line) exceeds P_{Loss} (blue dashed line), i.e. positive P_e in the I_p ramp-up phase. However, P_{Oh} (red solid line) and P_{Loss} (red dashed line) are overlapped in the failed case, hence P_e is zero. Figure 2(b), which is enlarged from Figure 2(a), shows that the behaviours of P_e in the burn-through phase are clearly different in the two cases. It should be noted that whether P_e in the I_p ramp-up phase is positive is determined by the change of P_e during the burn-through phase.

3. Radiation and Ionization Barrier (RIB) and Critical Degree of Ionization

The total electron power loss, P_{Loss} consists of the three power losses, i.e. radiation and ionization power loss P_{rad+iz} , equilibration power loss P_{equi} , and convective transport power loss P_{conv}^e . They are calculated as shown below [5][6].

$$P_{Loss} = P_{rad+iz} + P_{equi} + P_{conv}^e$$

$$P_{rad+iz} = V_p \times \mathcal{P}_{RI}(T_e) n_e n_D^0 \quad (3.1)$$

$$P_{equi} = V_p \times 7.75 \times 10^{-34} (T_e - T_i) \frac{n_e \ln \Lambda}{T_e^{3/2}} \left(\sum_A \sum_{z \geq 1} \frac{n_A^{z+} z^2}{M_A} \right), \quad (3.2)$$

$$P_{conv}^e = V_p \times \frac{3}{2} \frac{n_e e T_e}{\tau_e}, \quad (3.3)$$

where n_D^0 is a deuterium atom density, n_A^{z+} is an ion density of which the electric charge is $z+$, V_p is a plasma volume, M_A is an ion mass in [amu], τ_e is the electron particle confinement time, and $\mathcal{P}_{RI}(T_e)$ is the power coefficient of radiation and ionization, obtained from ADAS data [9].

In contrast to P_{equi} and P_{conv}^e , which are proportional to n_e , P_{rad+iz} has the maximum value at a certain degree of ionization since n_D^0 decreases as n_e increases. The peak value of P_{rad+iz} is defined as the *Radiation and Ionization Barrier* (RIB), and the degree of ionization at the RIB is defined to be the *Critical Degree of Ionization* for plasma burn-through, $\gamma(t_{RIB})$.

The RIB is of crucial importance since the required P_{Oh} for I_p ramp-up is mainly determined by the RIB. As will be seen, the magnitude of P_{rad+iz} is dominant in P_{Loss} during the burn-through phase. This implies that P_{Loss} has the maximum value at $\gamma(t_{RIB})$. Hence, once the P_{Oh} exceeds the P_{Loss} maximum, P_{Loss} decreases significantly as ionizations proceed. This enables T_e to increase, so that ionizations continue to proceed up to 100%.

In the burn-through phase, the density of deuterium atom $n_D^0(t)$ decreases as ionizations proceed, thereby increasing $n_e(t)$. If the deuterium atom density within a plasma volume decreases, neutral particles flow into the plasma volume from the ex-plasma volume, giving a dynamic fuelling effect. This effect impedes the decrease in neutral density within a plasma volume as much as the ratio of plasma volume to total neutral volume (= Vessel volume V_V). The reduction of neutral density in V_p is $\frac{V_p}{V_V}n_e(t)$. Hence, in the case that the deuterium recycling coefficient Y_D^D is 1 without gas pumping and puffing, n_D^0 in Equation (3.1) is

$$n_D^0(t) = n_D^0(0) - \frac{V_p}{V_V}n_e(t). \quad (3.4)$$

where $n_D^0(0)$ indicates the initial density of deuterium atom, which is proportional to the prefill gas pressure. By substituting n_D^0 in Equation (3.1) with $n_D^0(t)$ in Equation (3.4), $P_{rad+iz}(t)$ can be written as a negative quadric function of $n_e(t)$,

$$\begin{aligned} P_{rad+iz}(t) &= V_p \mathcal{P}_{RI}(T_e) n_e(t) \left(n_D^0(0) - \frac{V_p}{V_V} n_e(t) \right) \\ &= V_p \mathcal{P}_{RI}(T_e) \left(\frac{V_V n_D^0(0)^2}{4V_p} - \frac{V_p}{V_V} \left(n_e(t) - \frac{V_V n_D^0(0)}{2V_p} \right)^2 \right) \end{aligned} \quad (3.5)$$

Therefore, as ionizations proceed, $n_e(t)n_D^0(t)$ varies as shown in Figure 3(a) and has the maximum value,

$$\frac{V_V n_D^0(0)^2}{4V_p} \quad (3.6)$$

when $n_e(t)$ is equal to

$$\frac{V_V n_D^0(0)}{2V_p}. \quad (3.7)$$

The power coefficient $\mathcal{P}_{RI}(T_e)$ is a function of T_e as shown in Figure 4(b). The product of $n_e(t)n_D^0(t)$ and $\mathcal{P}_{RI}(T_e)$ results in the change of P_{rad+iz} , thereby the change of P_{Loss} in Figure 2. The increase in P_{Loss} during the I_p ramp-up phase in Figure 2 results from the increase in $\mathcal{P}_{RI}(T_e)$.

The degree of ionization in the burn-through phase can be calculated with

$$\gamma(t) = \frac{n_e(t)}{n_e(t) + n_D^0(t)}. \quad (3.8)$$

The degree of ionization at the RIB, $\gamma(t_{RIB})$, is then obtained by substituting $n_D^0(t)$

and $n_e(t)$ with Equation (3.4) and (3.7) as shown below.

$$\begin{aligned}\gamma(t_{RIB}) &= \frac{\frac{V_v n_d^0(0)}{2V_p}}{\frac{V_V n_d^0(0)}{2V_p} + \left(n_D^0(0) - \frac{V_p \frac{V_v n_d^0(0)}{2V_p}}{V_V} \right)} \\ &= \frac{V_V}{V_V + V_p}\end{aligned}\tag{3.9}$$

The plasma volume is limited by the vessel volume, i.e. $V_p \leq V_V$. This implies that $\gamma(t_{RIB})$ is always higher than 50%. In the case of JET, where V_V is $100[m^3]$ and initial plasma volume $V_p = 14.8[m^3]$ for a major radius $R = 3[m]$ and minor radius $a = 0.5[m]$, the critical degree of ionization $\gamma(t_{RIB})$ is 87.1%.

The simulation result of P_{rad+iz} are shown in Figure 4(a). P_{rad+iz} in the successful I_p ramp-up case (blue) has a maximum and decreases abruptly after the peak. This is consistent with Equation (3.5), since $n_e n_D^0$ decreases with increasing n_e after the peak point as shown in Figure 3(a). P_{rad+iz} falls with increasing degree of ionization from $0.08[s]$, t_{RIB} , when the critical degree of ionization is achieved. Accordingly, T_e begins to increase from t_{RIB} , and the increase becomes steep after P_{rad+iz} falls sufficiently around $0.015[s]$ as shown in Figure 4(c). Because the neutral particles are strong sinks of electron energy, the increase in T_e is impeded until the neutrals are sufficiently ionized.

As shown in Figure 4(b) the degree of ionization in the successful case (blue) approaches 100% over 87.1% which is the $\gamma(t_{RIB})$ calculated using Equation (3.9). On the other hand, the degree of ionization in the failed case does not exceed 87.1%. Hence, P_{rad+iz} does not fall abruptly, and P_e approaches 0, thereby resulting in the failure of the I_p ramp-up.

4. Criterion for Plasma Burn-through

4.1. Prefill gas pressure effects on RIB

Figure 5 shows simulation results of (a) plasma current, (b) degree of ionization, and (c) electron power losses for different prefill gas pressures. I_p ramp-up is delayed until almost 100% degree of ionization is achieved at the low prefill gas pressures (1×10^{-5} , 3×10^{-5} , and $5 \times 10^{-5}[Torr]$), and the delay increases with increasing prefill gas pressures. I_p ramp-up fails at a prefill gas pressure over $7 \times 10^{-5}[Torr]$. This indicates that for a prefill gas pressure of $7 \times 10^{-5}[Torr]$ and above the given loop voltage is not sufficient to achieve the critical degree of ionization, $\gamma(t_{RIB})$, as shown in Figure 5(b). The critical prefill gas pressure for the plasma burn-through with the given $20[V]$ loop voltage exists between $5 \times 10^{-5}[Torr]$ and $7 \times 10^{-5}[Torr]$.

As shown in Figure 5(b), I_p increases at the low pressures, hence the peak values of P_{rad+iz} shown at the low pressures in Figure 5(c) indicate the RIB, which increases with increasing prefill gas pressure as shown in Figure 5(c). Since neutrals are strong radiators, the larger number of neutrals at a high prefill gas pressure results in higher

P_{rad} . In addition, at a high prefill gas pressure, there are more neutrals to be ionized, thereby increasing P_{iz} .

The increase in RIB at the high prefill gas pressure can also be seen in Equation (3.5). Equation (3.5) implies that the maximum $P_{rad+iz}(t_{RIB})$ is

$$P_{rad+iz}(t_{RIB}) = \frac{V_V \mathcal{P}_{RI}(T_e) n_D^0(0)^2}{4}. \quad (4.1)$$

As shown in Equation (4.1), $P_{rad+iz}(t_{RIB})$ is proportional to the square of the initial density of deuterium atom $n_D^0(0)$. $n_D^0(0)$ is proportional to the prefill gas pressure p , hence $P_{rad+iz}(t_{RIB})$ is also proportional to the square of p under an identical T_e at the t_{RIB} . Since \mathcal{P}_{RI} is a function of T_e , a numerical calculation is required to calculate $P_{rad+iz}(t_{RIB})$.

In Figure 5(c), P_{iz+rad} is dominant in P_{Loss} during the burn-through phase, and the peak of P_{Loss} coincides with the RIBs. Therefore, the required electric field for plasma burn-through is mainly determined by the P_{iz+rad} .

4.2. Impurity effects on RIB

Impurities results in a significant increase in P_{iz+rad} during the plasma burn-through phase. In order to calculate RIB with impurities in the plasma, Plasma Surface Interaction(PSI) effect should be modelled in the numerical calculations.

The DYON code for plasma burn-through in the carbon wall JET has been validated, showing good agreement with the experimental data[6]. For the carbon wall, chemical sputtering is dominant, and the chemical sputtering yield is weakly dependent on the incident ion energy[10]. Hence, the sputtering yields in the carbon wall JET are assumed to be constants. In the case of oxygen ions, they are recycled as a monoxide, CO , at the wall with a sputtering yield close to 1[11]. Oxygen sputtering is also included for the carbon wall JET. The details of the sputtering model used in this article are in [6].

The effect of beryllium sputtering due to a deuterium or beryllium ions is important for JET experiments after the ITER-Like Wall(ILW) project where the first wall components are replaced to beryllium. For the beryllium wall, physical sputtering is dominant due to its low threshold energy[12]. A physical sputtering yield is a function of incident ion energy and the formulae have been given in [13],[14].

The Bohdanský formula for physical sputtering yield[13] is given as

$$Y = Q \times S_n(\epsilon) \times g(\delta) \quad (4.2)$$

where Q is yield factor and S_n is nuclear stopping cross-section which is given by

$$S_n = \frac{3.441\sqrt{\epsilon} \ln \epsilon + 2.718}{1 + 6.355\sqrt{\epsilon} + \epsilon(6.882\sqrt{\epsilon} - 1.708)}. \quad (4.3)$$

ϵ is defined to be E_0/E_{TF} where E_0 and E_{TF} are the ion wall-impacting energy and the Thomas-Fermi energy, respectively[13],[14]. The ion wall-impacting energy E_0

can be calculated as $2eT_i + 3eT_e$, assuming that ion's energy gain within a sheath is approximately $3eT_e$ [15]. The function $g(\delta)$ is defined to be

$$g(\delta) = (1 - \delta^{2/3})(1 - \delta)^2, \quad (4.4)$$

where δ is defined to be E_{th}/E_0 [15]. E_{th} indicates the threshold energy for physical sputtering. In the case of a deuterium and a beryllium ion bombardment on a beryllium target, the parameters required to calculate beryllium sputtering yields are given in Table 2. Since beryllium is an effective oxygen getter[8], oxygen should be small enough to ignore in the ILW. Based on this, the oxygen content is assumed to be 0 in the predictive simulations.

The simulation results of the RIB in JET are shown in Figure 6. In the case of the carbon wall, the second peak represents the RIB for carbon burn-through. As can be seen in Figure 6, the RIB for carbon burn-through is critical for I_p ramp-up since it is much higher than the RIB for deuterium burn-through. However, the RIB for beryllium burn-through does not appear. Hence, in the beryllium wall, the RIB for deuterium burn-through is the only RIB to be overcome for I_p ramp-up. This is due to the relatively low atomic number of beryllium, thereby resulting in low power coefficient \mathcal{P}_{RI} compared to carbon. Furthermore, the physical sputtering yields are also low due to the low T_e during the deuterium burn-through phase. Therefore, the burn-through criterion in the ILW will be reduced compared to the carbon wall experiments.

4.3. Criterion for plasma burn-through

The cyan solid lines in Figure 7 are the minimum electric field for plasma break-down, drawn analytically by using the Townsend criterion in Equation (1.1). The Townsend criterion shows that there is an optimum range of prefill gas pressure where the lowest toroidal electric field is available.

The black, red, and blue solid lines in Figure 7 represent the simulated minimum electric field for plasma burn-through without or with impurities. For the simulation, plasma minor radius is assumed to be $0.9[m]$. Other conditions assumed in the simulation is the same in Table 1. The required electric field for plasma burn-through increases monotonically as prefill gas pressure rises since the RIB is greater at a high prefill gas pressure.

In tokamak experiments, there can be significant impurity influx from the wall[4]. If the Plasma Surface Interaction (PSI) effect is included, the required electric field for plasma burn-through would be higher, thereby reducing the operation space available. As shown in Figure 6, the RIB for carbon burn-through is much greater than for deuterium burn-through. Hence, the required loop voltage in the carbon wall is significantly higher than for pure deuterium plasma. This results in the smaller operation space available in the carbon wall as shown in Figure 7. However, the RIB for beryllium burn-through is not significant as shown in Figure 6, and the RIB for deuterium burn-through is similar with the RIB calculated assuming pure deuterium plasma. This implies less loop voltage would be available for plasma burn-through in

the ILW, i.e. larger operation space available compared to the carbon wall as shown in Figure 7.

The recycling coefficients and the sputtering yields in the carbon wall JET can vary due to the effects of deuterium retention and carbon migration in the wall. In addition, the ratio of the plasma volume to the vessel volume, which is related to dynamic neutral gas fuelling from the ex-plasma volume as shown in Equation (3.4), is also different in each discharge shot. The criterion for plasma burn-through is also appeared to be changed with different conditions in the DYON code, i.e. steeper with higher recycling coefficient(or sputtering yield) or smaller plasma volume.

CONCLUSION

When determining the tokamak operation condition such as a prefill gas pressure, loop voltage, and magnetic stray field, the Townsend criterion is generally used. However, the Townsend criterion is the condition only for electron avalanche, i.e. the plasma breakdown. In order for I_p to increase, successful burn-through of deuterium and impurities is also necessary.

In this article, key aspects of the physics in the burn-through phase are investigated with the DYON code. The criterion for plasma burn-through is explained with the Radiation and Ionization Barrier(RIB) and the critical degree of ionization $\gamma(t_{RIB})$ obtained through an analytical derivation. Once the critical degree of ionization is achieved, ionization of neutrals can proceed up to 100% degree of ionization, thereby resulting in the increase in I_p . Hence, P_{OH} must exceed P_{Loss} maximum at $\gamma(t_{RIB})$.

The P_{Loss} maximum is dominated by the RIB. Since the RIB increases with the increasing prefill gas pressure, the required loop voltage is also high at the high prefill gas pressure. The required electric field for plasma burn-through is calculated by the DYON code, and the operation space available for JET is computed. The limitations set by the burn-through criterion will reduce the operational space with respect to those based on the Townsend criterion for an electron avalanche.

The RIB is significantly affected by plasma surface interaction. According to the simulation results of the DYON code, the PSI effects result in much smaller operation space for the carbon wall than for pure deuterium plasma. However, the RIB in the ILW is not much higher than in pure deuterium plasma. This results in larger operation space available for successful plasma initiation in the ILW than in the carbon wall.

Modelling of the evolution of plasma volume and sophisticated PSI treatments including the effects of deuterium retention and beryllium migration is required for a quantitative computation of the operation space available for ITER start-up.

ACKNOWLEDGEMENT

This research was funded partly by the Kwanjeong Educational Foundation and by the European Communities under the contract of Association between EURATOM and CCFE. The views and

opinions expressed herein do not necessarily reflect those of the European Commission. This work was carried out within the framework of the European Fusion Development Agreement.

REFERENCES

- [1]. Plasma Control ITER Physics Expert Group on Disruptions, MHD, Heating ITER Physics Expert Group on Energetic Particles, Current Drive, ITER Physics Expert Group on Diagnostics, and ITER Physics Basis Editors, Chapter 8: Plasma operation and control. *Nuclear Fusion*, **39**(12):2577, 1999.
- [2]. A. Tanga et al , Start-up of the ohmic phase in JET, In Heinz Knoepfel, editor, Tokamak Start-up, volume **26**, page 159. European Physical Society, Plenum Press, 1986.
- [3]. B. Lloyd et al , Low voltage ohmic and electron cyclotron heating assisted start-up in D3D, *Nuclear Fusion*, **31**:2031–2053, 1991.
- [4]. Y. Gribov et al , Chapter 8: Plasma operation and control, *Nuclear Fusion*, **47**(6):S385–S403, 2007.
- [5]. B. Lloyd et al , Ecrh-assisted start-up in ITER, *Plasma Physics and Controlled Fusion*, **38**(9):1627, 1996.
- [6]. Hyun-Tae Kim et al , Enhancement of plasma burn-through simulation and validation in JET, *Nuclear Fusion*, submitted, 2012.
- [7]. R. Papoular, The genesis of toroidal discharges, *Nuclear Fusion*, **16**:37–45, February 1976.
- [8]. J. Wesson, Tokamaks, Clarendon Press Oxford, 2004.
- [9]. H. P. Summers et al , Ionization state, excited populations and emission of impurities in dynamic finite density plasmas: I. the generalized collisional radiative model for light elements, *Plasma Physics and Controlled Fusion*, **48**(2):263, 2006.
- [10]. B.V. Mech et al , Isotopic effects in hydrocarbon formation due to low-energy h+/d+ impact on graphite, *Nuclear Materials*, **255**(2-3):153 – 164, 1998.
- [11]. J.W. Davis et al , Impurity release from low-z materials under light particle bombardment, *Nuclear Materials*, **241-243**:37 – 51, 1997.
- [12]. M.F. Stamp et al , Experience of Beryllium Sputtering Yields on JET, San Diego, California, USA, May 2010. the 19th International Conference on Conference on Plasma Surface Interactions.
- [13]. C. Garcia-Rosales et al , Revised formulae for sputtering data, *Nuclear Materials*, **218**(1):8 – 17, 1995.
- [14]. Y. Kudriavtsev et al , Calculation of the surface binding energy for ion sputtered particles, *Applied Surface Science*, **239**(3??):273 – 278, 2005.
- [15]. P.C. Stangeby, The Plasma Boundary of Magnetic Fusion Devices, Institute of Physics Publishing Bristol and Philadelphia, 1999.

Initial electron temperature	$T_e(0)$	1[eV]
Initial ion temperature	$T_i(0)$	0.03[eV]
Initial degree of ionization	γ	0.002
Deuterium sputtering yield	Y_D^D	1
Plasma major radius	R	3[m]
Plasma minor radius	a	0.5[m]
Internal inductance	l_i	0.5
Loop voltage	V_l	20[V]
Vacuum vessel volume		100[m ³]

Table 1: Plasma parameters assumed for the burn-through simulation.

Incident ion on Be target	D	Be
E_{th} [eV]	9	25
E_{TF} [eV]	282	2208
Q	0.1566	0.7517

Table 2: Parameters for beryllium sputtering due to a deuterium or beryllium ion bombardment.

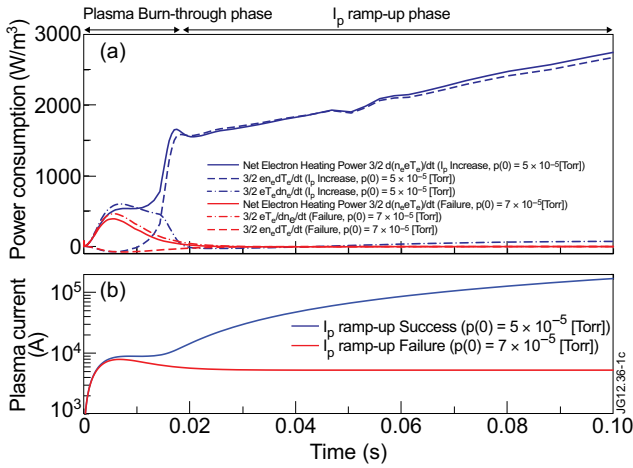


Figure 1: The colors of lines in (a) and (b) indicate successful I_p ramp-up (blue) and failure (red). The solid lines represent the net electron heating power P_e . The dashed lines and the chain lines are the amount of P_e consumed by increasing T_e and increasing n_e , respectively. The corresponding plasma currents I_p are represented by the blue solid line (I_p ramp-up) and the red solid line (non sustained break-down) in (b). In order for I_p to increase, P_e must be positive in the I_p ramp-up phase.

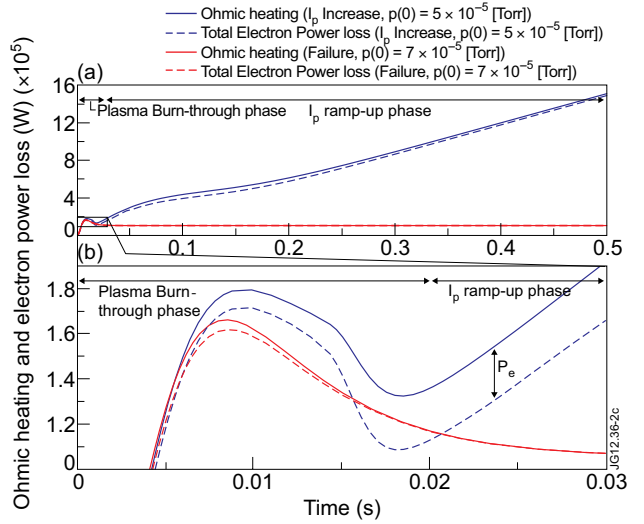


Figure 2: The solid lines and the dashed lines in (a) show P_{Oh} and P_{Loss} in successful (blue) and failure (red) cases, respectively. (b) is an enlarged figure from the burn-through phase in (a). Whether the net electron heating power is positive in the I_p ramp-up phase is determined in the burn-through phase.

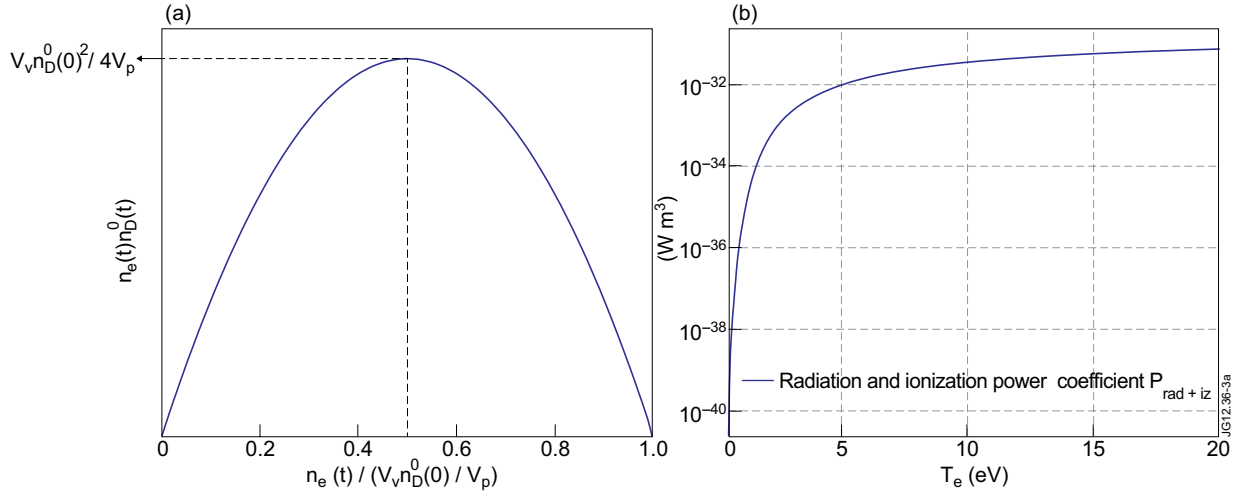


Figure 3: As shown in (a), $n_e n_D^0$ can be substituted by $n_e(t)(n_D^0(0) - n_e(t))$ in the case of a recycling coefficient ($= 1.0$). Therefore it has a maximum value as $n_e(t)$ approaches Equation (3.7). P_{RI} is strongly dependent only on T_e as shown in (b). The combined term $n_e n_D^0 P_{RI}$ behaves as in Figure 4(a).

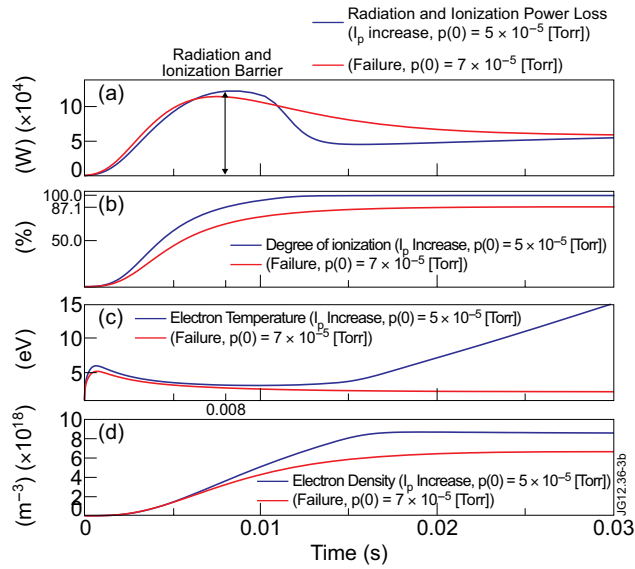


Figure 4: The blue line and the red line in (a) indicate the case of successful I_p ramp-up and failed ramp-up, respectively. (a) shows P_{rad+iz} . The corresponding degree of ionization is indicated in (b). The critical degree of ionization $\gamma(t_{RIB})$ is 87.1% as calculated using Equation (3.9). Whether or not a degree of ionization can go over $\gamma(t_{RIB})$ is critical for I_p ramp-up. (c) and (d) describes electron temperature and density, respectively.

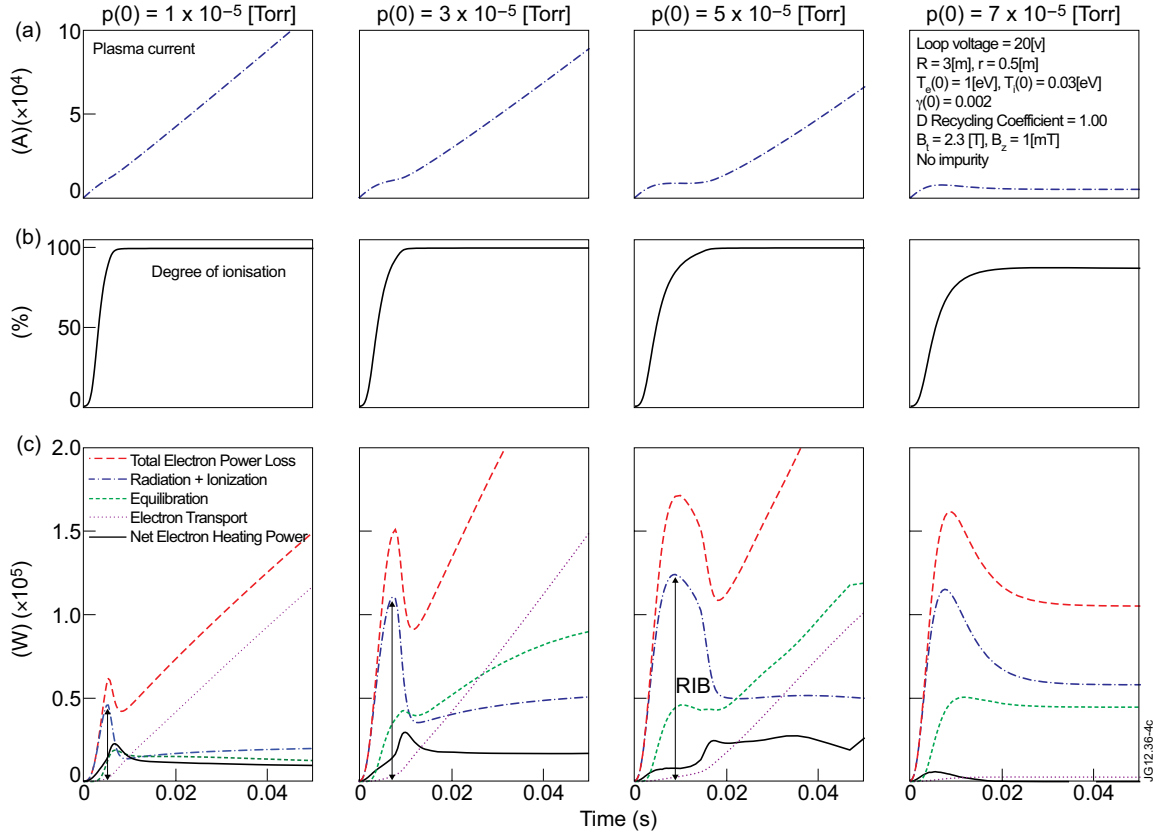


Figure 5. The figures show (a) the plasma current, (b) the degree of ionization, and (c) various electron power losses at different prefill gas pressures, 1×10^{-5} , 3×10^{-5} , 5×10^{-5} , and 7×10^{-5} [Torr]. The assumed loop voltage and plasma parameters are shown in Table 1. Under the given condition, a critical prefill gas pressure for I_p rampup exists between 5×10^{-5} and 7×10^{-5} [Torr]. Prefill gases are almost fully ionized in the cases of successful I_p ramp-up while they are not fully ionized in the cases of failure. The colored solid lines in (c) indicate P_{Loss} (red), P_{equi} (green), P_{conv} (cyan), and P_{rad+iz} (blue), respectively. As shown in (c), P_{rad+iz} is dominant in P_{Loss} during the burn-through phase, and its peak values coincide the RIB. The RIB increases with increasing prefill gas pressure. Therefore, the higher the prefill gas pressure, the larger the maximum for P_{Loss} .

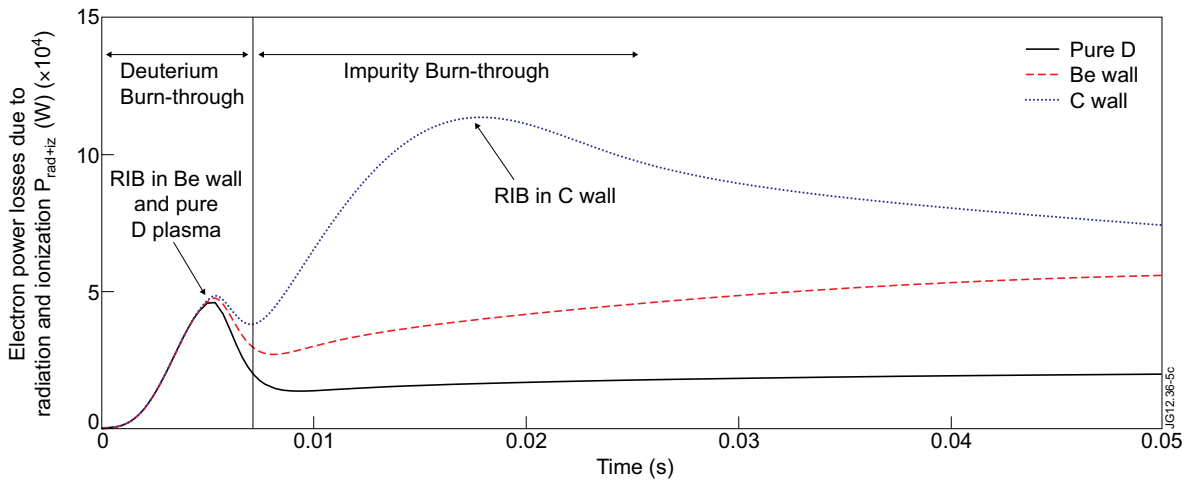


Figure 6: Each line indicates the radiation and ionization power losses in carbon wall (blue), beryllium (red), and pure deuterium plasma (black). In the case of carbon wall, the RIB is determined by the second peak, which results from carbon.

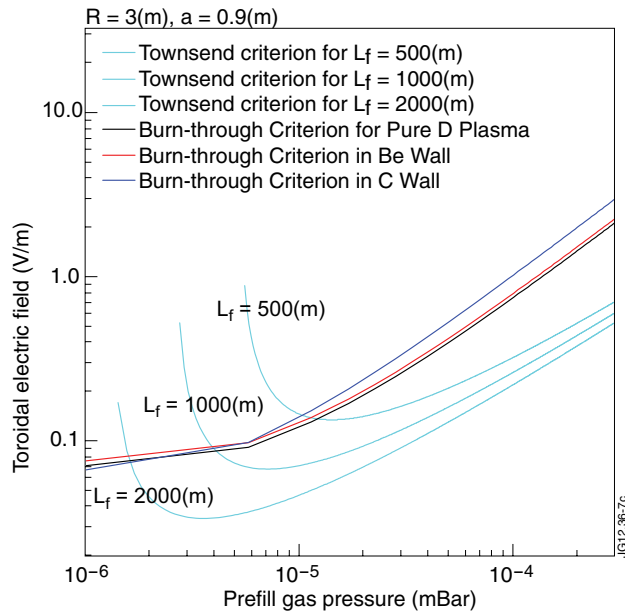


Figure 7: The cyan solid lines show the Townsend criterion at different effective connection lengths, as indicated with 500, 1000, and 2000[m], respectively. The black, red, and blue solid lines indicate the burn-through criterion, i.e. the minimum electric field for plasma burn-through in the case of pure deuterium plasma (black), beryllium wall (red), and carbon wall (blue), respectively. For the burn-through simulation, the major radius and minor radius of the plasma are assumed to be 3[m] and 0.9[m]. The area above both the burn-through criterion and Townsend criterion represents operation space available for successful start-up in JET.